Model/Data Fusion: Developing Bayesian Inversion to Constrain Equilibrium and Mode Structure

M.J. Hole 1), G. von Nessi 1), J. Svensson 2), J. Bertram 1), D. Pretty 1), L. C. Appel 3), B. Blackwell 1), J. Howard 1), R. Dewar 1)
1) Plasma Research Laboratory, Australian National University, ACT 0200, Australia
2) Max Planck Institute for Plasma Physics, Teilinstitut Greifswald, Germany.
3) Euratom/Culham Centre for Fusion Energy, Abingdon, Oxon OX143DB, UK.
E-mail contact of main author: matthew.hole@anu.edu.au

Abstract. Recently, Bayesian probability theory has been used at a number of experiments to fold uncertainties and interdependencies in the diagnostic data and forward models, together with prior knowledge of the state of the plasma, to increase accuracy of inferred physics variables. A new probabilistic framework, MINERVA, based on Bayesian graphical models, has been used at JET and W7-AS to yield predictions of internal magnetic structure. A feature of the framework is the Bayesian inversion for poloidal magnetic flux without the need for an explicit equilibrium assumption. We discuss results from a new project to develop Bayesian inversion tools that aim to (1) distinguish between competing equilibrium theories, which capture different physics, using the UK MAST spherical tokamak; and (2) test the predictions of MHD theory, particularly mode structure, using the Australian H-1 Heliac.

1. Introduction

Due principally to neutral beam heating, several tokamak experiments now boast plasma toroidal rotation speeds that approach the thermal Mach speed and have significant stored energy (~25% of total stored energy [1]) residing in the energetic particle population produced by charge exchange with thermals. Despite this, single-fluid thermalised ideal MHD is still the foundation of nearly all equilibrium analysis. Detailed magnetic reconstruction based on this treatment ignores the energetic complexity of the plasma, and can result in model-data inconsistencies, such as thermal pressure profiles which are inconsistent with the total stored kinetic energy of the plasma. Motivated by the omission of this physics, a range of new descriptions have emerged that include thermal rotation and energetic particles [2]. Such models are often constrained by quasi-variables user input profiles which are a complicated function of the measured data.

A parallel development has been the improvement in the diversity, accuracy and resolution of plasma diagnostics. Often, interpretation requires a detailed knowledge of the plasma equilibrium. For example, inference of the toroidal current profile $j_\varphi(\psi)$ from line of sight measurements of the polarization angle requires a knowledge of the poloidal flux ψ across the plasma. Formally, diagnostic forward functions relate the vector of plasma parameters I to the measurement vector D. For a linear system, such as toroidal current inference, I and D are normally related through a response matrix M with additional contributions C, such that D = MI+C. Inference involves inverting this relationship to give plasma parameters I that are consistent with the data D. A widespread technique used is least-square fitting, in which prior assumptions are included via a penalty term in the fit. One limitation of this technique is the handling of uncertainties: normally done by selecting different data sets and repeating the inference procedure to produce a standard deviation. This approach assumes the underlying probability distribution function of the data to be Gaussian. A second limitation is that uncertainties stemming from parameter interdependency in the data or plasma parameters is not made explicit, and so the source of uncertainty in the final inference is not resolved.

The confluence of increased performance plasmas with improved diagnostic resolution can lead to inconsistencies between data and equilibrium model. An example is filamentation of flux surfaces in the Rijhnuizen Tokamak, which was inferred from fluctuations in measurements of electron temperature. [3] Subsequent analysis of the Thomson scattering detection chain revealed that with the correct photoelectron statistics and 2D instrument profile, similar structures could arise from noise. [4] Examples such as this, as well as the development of new force balance models, suggest inference framework is needed to capture uncertainties when forming plasma profiles, and to verify different equilibrium models. Such a framework may also offer the possibility to infer otherwise difficult to diagnose properties, such as the energetic particle pressure.

The Bayesian approach to inference in fusion plasmas, developed by multiple authors, [5,6,7] involves the specification of an initial prior probability distribution function (pdf), P(I), which is then updated by taking into account information that the measurements provide through the likelihood pdf P(D|I). The result is the posterior distribution P(I|D) given by Bayes' formula

$$P(I \mid D) = P(D \mid I)P(I) / P(D). \quad (1)$$

The advantage of the Bayesian approach over traditional inversion techniques is two-fold: (i) prior knowledge, including known parameter inter-dependencies is made explicit, and (ii) as the formulation is probabilistic, random errors, systematic uncertainties and instrumental bias are integral part of the analysis rather than an afterthought.

We have implemented Bayesian inversion using the MINERVA framework. [8] Within this framework, probabilistic graphical models are used to project the dependence of the posterior distribution function on the prior, the data, and the likelihood. An advantage of this approach is that it visualises the complex interdependency between data and model, and thus expedites model development.

In previous work we have reported on development of MINERVA for toroidal current tomography in MAST, folding together the vacuum toroidal field, pickup coil data, flux loops, and the polarisation angle of emitted light from neutrally excited species during neutral beam injection due to the Motional Stark Effect. [9] One valuable piece of information poloidal flux inference provides is the safety factor or q profile and its associated uncertainty. We have also corrected the vacuum toroidal field to account for poloidal currents by using the static-plasma Grad-Shafranov equation as a constraint, folding in measurements of the toroidal current density and pressure gradient modelled outside of MINERVA [9,10], and inferring the toroidal magnetic flux function. This work showed that the inclusion of a poloidal current model for MAST yields a 5% increase in q on axis, and a 5% decrease in q at the edge. The inclusion of a diamagnetic loop in the MINERVA framework, together with a toroidal flux function model, enabled the extraction of poloidal currents internal to MINERVA [11] Although promising, these results showed sensitivity to the prior, and the use of iteration meant that uncertainties could no longer be generated, and a different approach is now under consideration. In other work, we have shown how Tikhonoff regularisation combined with diagnostic cross-validation can be combined to form a new technique, "Tikhonoff Cross-Validation", used to remove systematic uncertainties. [12]

In 2010 we have developed Bayesian inference models for electron temperature and pressure from Thomson scattering data, as well as the inference of ion temperature and ion thermal flow from charge exchange recombination data. In this work we present first results on the modelling and Bayesian inference of electron temperature T_e, electron density n_e, ion temperature T_i and ion flow velocity v_i from Thomson Scattering and Charge Exchange

recombination data. For the 22nd IAEA Fusion Energy Conference, we intend to update inference for the toroidal magnetic flux function for a flowing plasma, using inferences of n_e, T_e, T_i, and v_i from MINERVA. A wider equilibrium modelling objective of the Bayesian project is build a verification framework to test the degree to which the Grad-Shafranov equation and more detailed force balance models describe the plasma.

A second objective of our project is to develop Bayesian inversion for mode structure. The low beta H-1 heliac plasma is an ideal environment in which to develop these tools, as the plasma exhibits a rich spectrum of fluctuation activity [13], and the equilibrium configuration is close to the vacuum field, and so sources of uncertainty in the mode structure and frequency are principally derived from the density, temperature, or resistivity profile, not the field structure. To this end we report on two developments (1) construction of a forward model for the interferometer and imaging Doppler spectroscopy system for H-1 plasmas, and its implementation into the MINERVA framework, and (2) implementation of a Bayesian inference procedure for mode numbers and frequency using a reduced cylindrical model. [9, 14]

2. Bayesian current tomography in MAST

Our development of Bayesian inference of the current profile on MAST, detailed in Hole *et al* [9], closely follows the seminal work of Svensson and Werner [15]. In that work, the plasma was represented as a grid of toroidal axis-symmetric current beams, each with rectangular cross-section and each beam carrying a uniform current density. In the Mega Ampére Spherical Tokamak MAST, we have placed these beams so as to fill-out the entire plasma volume, including regions outside the last closed flux surface up to the vacuum poloidal field coils. The magnetic field generated is then a summation of Biot-Savart's law over current beams.

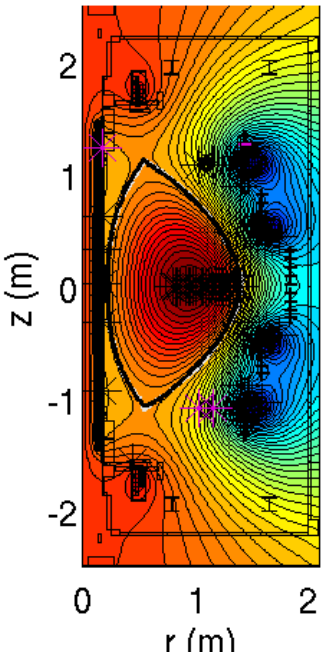

Figure 1 : Poloidal flux surfaces inferred for MAST shot # 24600 at 280ms using pickup coils, flux loops and MSE. The solid black and white lines are the EFIT and Bayesian-inferred last closed flux surfaces, respectively.

Here, we build on the results of Hole *et al* [10], who showed current tomography and q profiles computed using MINERVA for discharge #22254. Figure 1 shows poloidal flux surfaces from MAST discharge #24600 at 280 ms using pickup coils, flux loops and MSE data. Discharge #24600 is a deuterium plasma in a double-null configuration, which was heated with 3 MW of neutral beam heating and a plasma current of I_p = 0.8 MA. The time of 280ms analyzed here is the high-resolution TS time closest to the peak β. The figure shows a contour plot of $\psi(R,Z)$, which is calculated from the maximum of the posterior of the distribution of toroidal current beams. Overlaid on the contours are traces of the poloidal field coil cross sections and conducting surface cross sections for the MAST experiment, as well as the last closed flux surface calculated from the plasma beam model and the corresponding EFIT last closed flux surfaces. One outcome of the Bayesian approach is generation of pdfs of inferred quantities from which the uncertainty can be inferred. For instance, Fig. 2 shows the corresponding safety factor or *q* profile and its uncertainty.

In Bayesian inference, the uncertainty in an inferred parameter is computed by sampling different realizations from the (generally not analytically tractable) posterior. Here, we have

computed the *q* profile for each realization of current beams across the plasma, and rendered the ensemble of samples as a histogram, where the shading represents the density of samples.

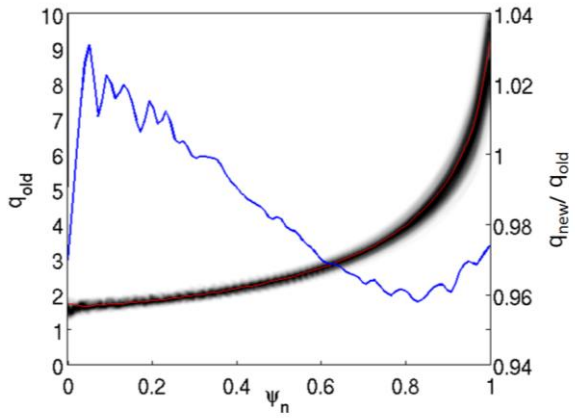

Figure 2: Safety factor *q* profile as a function of normalized poloidal flux found by sampling the posterior 200 times for shot #24600 at 320ms. The poloidal flux is normalized such that ψ_n=0 is the magnetic axis and ψ_n=1 is the edge. Also shown is q_{old}/q_{new} obtained by correcting the toroidal flux function to account for poloidal currents

As in Hole et al [10], we have the inference of the toroidal magnetic flux function by using the static-plasma Grad-Shafranov equation as a constraint, and folding in measurements of the toroidal current density and pressure gradient [9 ,10] and inferred the toroidal magnetic flux function. Replacing this in the vacuum field solution for MINERVA accounts for poloidal currents. The right axis of Fig. 2 shows the change in the q profile due to this correction.

2.1 Thomson Scattering and Charge Exchange Recombination Spectroscopy

We have implemented Bayesian inference for the Thomson Scattering diagnostic: Figure 3 shows a preliminary Bayesian inference for the expectation of electron density n_e and temperature T_e. Profiles for the density and temperature are similar to those extracted routinely from MAST using least squares fitting.

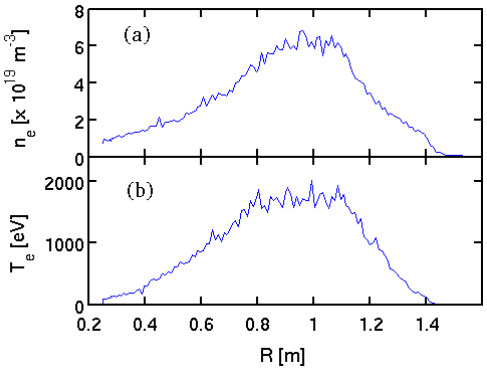

Figure 3: Bayesian inference of (a) n_e and (b) T_e from Thomson scattering system for 24600 at 280ms.

We have also implemented Bayesian inference for the Charge Exchange Recombination diagnostic. The forward model is based on the work of Wisse [16]. Figure 4 shows preliminary results of Bayesian inference for the expectation of ion density, ion temperature and ion flow speed parallel to line of sight at intersection with neutral beam. For this discharge, background subtraction was based on linear interpolation (in flux-coordinates) between the SouthWest (SW) neutral beam lines-of-sight and passive line-of-sight, and a new deconvolution algorithm written. The density profile is missing an absolute calibration, and so we have normalised it to the density at the static Grad-Shafranov magnetic axis, located at a major radius of 0.94m.

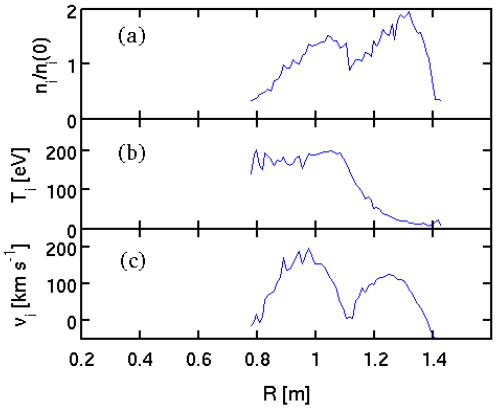

Figure 4: Bayesian inference of (a) n_i and (b) Ti and (c) flow speed vi parallel to line of intersection with neutral beam for discharge 24600 at 280ms.

3.0. A Bayesian approach to mode inference

A second objective of the project is to develop a Bayesian inversion tool to test predictions of MHD mode theory, particularly mode structure. We have pursued this task in H-1 plasmas by inference of the mode set H=(m,n,*f*) with m,n the poloidal and toroidal mode number, and *f* the frequency. In Sec. 3.1 we implement this approach on Mirnov coil data using a reduced cylindrical plasma model to produce prior MHD eigenfunctions. In Sec. 3.2, we report on development of Bayesian inference for density and temperature using a forward model for the H-1 interferometer and imaging Doppler spectroscopy system. This is complementary to inference of H, as the mode frequency is a function of the density profile.

3.1. Bayesian inversion for candidate modes in MINERVA

We have modelled H-1 plasmas using a stellarator normal-mode formulation [17], obtained by linearizing a set of stellarator ideal reduced MHD equations [18], neglecting toroidal effects. The model has been extended to incorporate a vacuum region, and used to compute Global Alfven Eigenmodes (GAEs) for the H-1 Heliac.[14] To quantify agreement to field oscillations at the H-1 poloidal Mirnov array, we have developed a Bayesian inference technique to contrast and compare between alternate GAE solutions. This represents a first attempt to statistically ascertain the confidence in the mode fit, as compared to alternate fits and the background field.

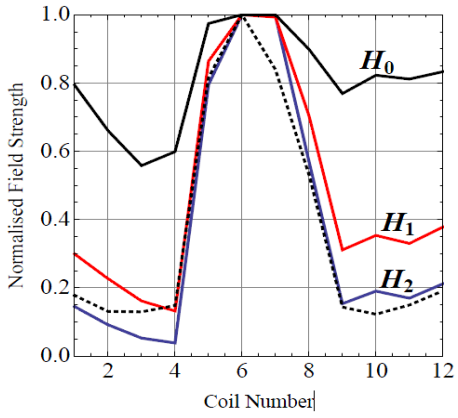

Figure 5. Normalised magnetic field strength of measured data (dashed) in H-1, two GAEs H_1 = {4, 5, 109.6 kHz} and H_2 = {7, 9, 19.7kHz},.and the equilibrium field H_0 = {0, 0, 0 kHz}, plotted against coil number. The measured data is a root-mean-square time average of poloidal Mirnov array data for discharge number 58063, which had current winding ratio κ_h=0.54.

Figure 5 shows three alternate candidate solutions, denoted H_0, H_1, and H_2 to describe the variation in fluctuation strength as a function of poloidal coil number for H-1. These solutions are the equilibrium field H_0= { 0,0,0 }, and the two cylindrical plasma GAE solutions H_1= { 4,5,109.6 kHz} and H_2= { 4,5,109.6 kHz}. Also shown is the measured data for discharge 58063, which had spectral peak at 37.4 kHz .

A Bayesian analysis requires us to compare and contrast between different solutions. To proceed, we construct the hypothesis space $\mathcal{H}$= {H_1, H_2, ,.... , H_n}, which is the set of candidate mode solutions about which we wish to make inferences, as well as the data space $\mathcal{D}$ = {D_1,D_2, ,.... , D_n}. We also require a forward model, $F: \mathcal{H} \rightarrow \mathcal{D}$, which gives us the expected data D corresponding to different hypotheses H. [14]

Assuming no prior knowledge, each hypothesis is equally likely, and our prior distribution is given by $P(H_0)=P(H_1)=P(H_2)=1/3$. As an illustration of the technique, we assume the error on the Mirnov coils is normal and independently distributed, with a variance of 0.1 on normalised measurements, and a standard deviation of 1kHz on the measured frequency. With these assumptions, the likelihood can be written $P(D|H_i)= \mathcal{N}(F(H_i,), \Sigma_0)|_D$, where i=0,1,2 and Σ_0=diag(a_1,a_2,...,a_{13}) with a_j=0.1 for j=1,2,...,12 and a_{13}=1. Here, $\mathcal{N}(\mu, \Sigma)$ denotes a normal distribution with mean vector μ and covariance matrix Σ. Applying Bayes formula, Eq. (1), we obtain $P(H_i|D)= \mathcal{N}(F(H_i,), \Sigma_0)|_D$ / 3P(D) for each hypothesis.

To obtain relative probabilities we evaluate the conditional distribution at the dataset D_{58063}, which is the root-mean-square time-averages of Mirnov array data from discharge 58063. Including frequencies in the solution sets H_0, H_1, and H_2 yields relative probabilities $P(H_0|D_{58063})\sim0$, $P(H_1|D_{58063})\sim0$ and $P(H_2|D_{58063})\sim1$, thereby concluding the (m,n) = (7,9) mode is the solution. Ignoring frequencies yields $P(H_0|D_{58063})\sim0$, $P(H_1|D_{58063})\sim0.29$ and $P(H_2|D_{58063})\sim0.71$, which confirms the overall better fit visible in Fig. 5 for the (7,9) mode. In either case we can reject the null hypothesis.

While we have demonstrated Bayesian inference for the mode numbers and frequencies is possible, it offers little beyond visual inspection of competing solutions. A limitation of this technique is the small number of discrete candidate modes, as well as the disparate frequency and mode numbers of the different candidates. In ongoing work, we have refined our focus to study the Bayesian inference of radial mode structure from multiple diagnostics given mode numbers, frequencies, and taking as prior the radial envelope of the perturbed displacement from 3D ideal MHD code CAS3D [19].

3.2. Bayesian inversion of an interferometer and imaging Doppler spectroscopy system

In other work, we have also developed a forward model for the interferometer [20] and imaging Doppler spectroscopy system for H-1 plasmas, [21] and implemented it into MINERVA. In order to account for configuration dependent diagnostic lines of sight a VMEC [22] node has been developed which returns surface step profile for a given H-1 configuration. The forward model for the interferometer is simply a line integration over the configuration-dependent electron density step profile. The line intensity $I(T_e, n_e)$ is estimated by a coronal equilibrium model, and we restrict the analysis to estimation of T_e and n_e from simulated H_α and H_β lines over a single set of chords. For comparison with simulated data, the ratio $\mu_{0\alpha}/\mu_{0\beta}$ is used , in order to nullify calibration parameters common to both emission lines. Here, $\mu_{0\alpha}$ and $\mu_{0\beta}$ are the emission intensity of the two lines.

Simulated data is generated by using parabolic profiles, as shown in Fig. 6 with typical H-1 values at the plasma core $n_e=10^{18}$ m^{-3}, T = 20 eV. For the simulated interferometric data the Gaussian error has standard deviation $\sigma=10^{15}$ m^{-2}, corresponding to 4% signal strength at the edge line of sight and 0.3% at plasma core. The variation in $\mu_{0\alpha}/\mu_{0\beta}$ across the simulated lines of sight is only ~5% of the signal strength; in this case σ is ~ 1% of the variation.

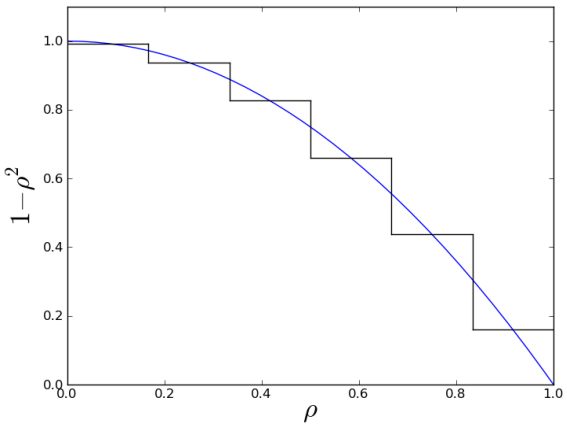

Figure 6: Synthetic radial profile data for n_e and T_e for typical H1 profiles (blue). The symbol ρ is a normalised density, with ρ=1 the plasma edge.

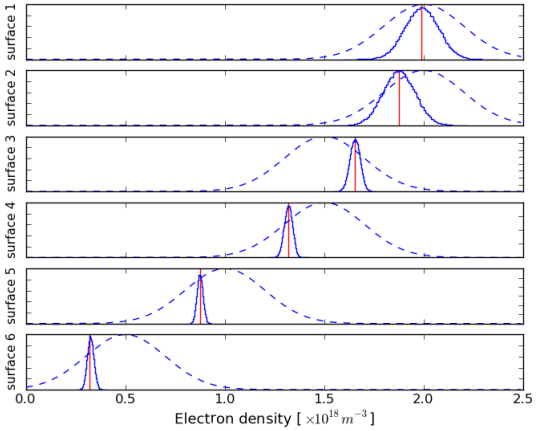

Figure 7: Bayesian inference for electron density n_e. The solid line is the posterior, the dashed line the prior

Posterior distributions for the extracted parameters were computed using Markov Chain Monte Carlo sampling. Figure 7 show the extracted posterior distribution function for n_e for the six steps, together with the synthetic values and prior distributions. Although these results are promising, there is an overall absolute calibration which is unknown in the experiment, preventing application to real H1 data. We plan to use build on this expertise to implement Bayesian inference of radial mode structure.

4.0 Conclusions

In this work we have described a Bayesian inversion framework for force balance and mode structure. For equilibrium modelling in MAST we have reported on development of Bayesian inference for six diagnostic systems: current tomography folding together poloidal pickup coils, MSE data and flux loops; Thomson Scattering, Charge Exchange Recombination, and the diamagnetic loop. We have also demonstrated these for a high performance MAST discharge. Using the inferred plasma parameters and the Grad-Shafranov equation, we have been able to infer the toroidal magnetic flux profile, and correct current tomography in MAST for poloidal currents. The correction produces a 3% increase in the on-axis safety factor, and a 4% decrease near the plasma edge. This correction exceeds the intrinsic uncertainty in the q profile of ~2%.

Motivated by the aim to resolve mode structure on H-1 using Bayesian inference, we have also introduced a Bayesian framework to select between competing mode choices, as computed by a reduced cylindrical model. While successful, we have shown that a limitation of this technique is the small number of discrete candidate modes, as well as the disparate frequency and mode numbers of the different candidates. In ongoing work, we plan to refine our focus to study the Bayesian inference of radial mode structure from multiple diagnostics given mode numbers, frequencies, and taking as prior the radial envelope of the perturbed displacement from 3D ideal MHD code CAS3D [19]. Finally, we have implemented Bayesian inversion for n_e, T_e, and T_i of synthetic data from a combined interferometer and imaging Doppler spectroscopy system. While the system was able to infer parameters near those synthesised, the technique requires the absolute calibration which is unavailable in the experiment. We plan to use build on this expertise to implement Bayesian inference of radial mode structure.

Acknowledgement: This work was jointly supported by International Science Linkages Grant CG130047, the Australian National University, the UK Engineering and Physical Sciences Research Council, Max-Planck-Institut fűr Plasmaphysik, and Euratom.

---

1 M J HOLE, R J AKERS, L C APPEL, R J BUTTERY, C BRICKLEY, N J CONWAY, M GRYAZNEVICH, T C HENDER, O J KWON, M VALOVIC, S MEDVEDEV, A PATEL, S SAARELMA, D TAYLOR, H R WILSON, THE MAST TEAM, "Ideal MHD stability of the mega-ampere spherical tokamak", Plas. Phys. Con. Fusion **47**,581–613, 2005

2 M. J. HOLE, G.DENNIS, Plas. Phys. Con. Fus., **51**, 035014, 2009

3 N. J. L. CARDOZO *et al*, Phys. Rev. Lett, 73, 256, 1994

4 N. J. L. CARDOZO *et al*, Phys. Rev. Lett **90**, 0031, 2003

5 G. A. COTTRELL, in "Maximum Entropy in Action", edited by B. Buck and V. A. Macaulay (Oxford Science, Oxford, 1990).

6 R. FISCHER, A. DINKLAGE, E. PASCH, Plas. Phys. Cont. Fus. 45, 1095 (2003).

7 J. SVENSSON *et al.*, Rev. Sci. Instrum. 75, 4219, 2004.

8 J. SVENSSON, A. WERNER, IEEE Int. Symposium on Intelligent Signal Processing WISP, Otcober 2007.
9 M. J. HOLE, G. VON NESSI, J. BERTRAM, J. SVENSSON, L. C. APPEL, B. D. BLACKWELL, R. L. DEWAR, J. HOWARD, J. Plasma Fusion Research Series Vol. 9, pp 479-486, 2010.
10 M. J. HOLE, G. VON NESSI, D. PRETTY, J. HOWARD, B. BLACKWELL, J. SVENSSON, L. C. APPEL, "The use of Bayesian inversion to resolve plasma equilibrium", Rev. Sci Instrum, Accepted 03/08/2010.
11 L. C. APPEL, M. J. HOLE, J. SVENSSON, G. VON NESSI, THE MAST TEAM, "Bayesian Inference applied to Magnetic Equilibrium on MAST", P4-103**,** EPS 37th Conference on Plasma Physics, 21-25 June, Dublin 2010.
12 G. T. VON NESSI, M. J. HOLE, J. SVENSSON, L. APPEL, "Tychonoff Cross-Validation and Bayesian Inference of MAST Plasma Equilibria", submitted Plas. Phys. Con. Fusion, 07/09/2010.
13 D. G. PRETTY. A Study of MHD Activity in the H-1 Heliac Using Data Mining Techniques. PhD thesis, The Australian National University, 2007.
14 J. BERTRAM, M. J. HOLE, R. L. DEWAR, B. D. BLACKWELL, D. PRETTY "Global Alfvén Eigenmodes on the H-1 Heliac", submitted to Plas. Phys. Con. Fusion 11/08/2010
15 J. SVENSSON, A. WERNER, Plas. Phys. Con. Fus. 50: 085002, Jan 2008
16 M. WISSE, "Charge-Exchange Spectroscopy in the MAST Tokamak", PhD Thesis., University College Cork (Ireland)/ UKAEA Fusion, October 2007.
17 M.WAKATANI, T. TATSUNO. "Ideal interchange instabilities in stellarators with a magnetic hill", Nucl. Fusion, 39(10), 1999.
18 H. R. STRAUSS. "Stellarator equations of motion. Plasma Physics", 22(7), 1980.
19 C. NÜHRENBERG. "Compressional ideal magnetohydrodynamics: Unstable global modes, stable spectra, and Alfvén eigenmodes in Wendelstein 7X-type equilibria". Physics of Plasmas, 6(137), 1999.
20 J. HOWARD, D. OLIVER, "Electronically swept millimetre-wave interferometer for spatially resolved measurement of plasma electron density," Applied Optics, **45**, 2006.
21 J. HOWARD, C. MICHAEL, F. GLASS, A. DANIELSSON, "Time-resolved 2-D plasma spectroscopy using coherence imaging techniques", Plasma Phys. Control Fusion, **45**, 1143, 2003.
22 S. P. HIRSHMAN, W. I. VAN RIJ, P. MERKEL, Comput. Phys. Commun. **43**, 143, 1986.